5.10 DETECTION AND EVALUATION OF THE EFFECTS OF SPLIT FRONTS ON THE EVOLUTION OF APPALACHIAN COLD AIR DAMMING

Michael J. Brennan*
North Carolina State University, Raleigh, North Carolina

Steven E. Koch
Forecast Research Division, NOAA/OAR/FSL, Boulder, Colorado

Gary M. Lackmann
North Carolina State University, Raleigh, North Carolina

1. INTRODUCTION AND BACKGROUND

The Split Cold Front (SF) model presented by Browning and Monk (1982) and the Cold Front Aloft (CFA) model introduced by Hobbs et al. (1990) each mark a significant departure from the traditional thinking of how precipitation is distributed near a mid-latitude cyclone. The SF model involves low wet bulb potential temperature (θ_w) air in the 700hPa to 500hPa layer advecting above high θ_w in the surface warm sector at least 100 km ahead of the surface cold front (Browning and Monk 1992). Browning and Monk (1982) show that in numerous cases a rainband of at least moderate intensity occurred with the passage of the SF. The CFA model is similar, involving a mid-level baroclinic zone producing precipitation at the surface 200 to 300 km ahead of a surface trough (Hobbs et al. 1990). In fact, Hobbs et al. (1990) note that when the surface trough is a cold front, the CFA model reduces to the SF model. Several recent studies (Locatelli et al. 1998, Koch and Mitchem 2000; Koch 2001) have shown the importance of a CFA in the organization of precipitation ahead of the surface cold front.

Cold Air Damming (CAD) is characterized by cold air becoming trapped along the slopes of a mountain range (Richwein 1980). In the southeastern U.S. CAD occurs when cold air flowing from a surface anticyclone in the northeastern U.S. becomes blocked by the terrain and is forced southwestward along the eastern slopes of the Appalachians due to a force imbalance (Forbes et al. 1987). Many complex processes act to reinforce the shallow, stable cold air dome that develops, including upslope adiabatic flow (Keeter et al. 1995) and evaporative cooling in the subcloud layer (Bell and Bosart 1988, Fritsch et al. 1992). In addition, localized evaporative cooling may induce CAD in the absence of synoptic-scale support (Koch 2001). During CAD a coastal front (e.g. Bosart et al. 1972, Riordan 1990) often marks the boundary between the cold airmass over the continent and the warm maritime airmass over the Gulf Stream. The inland movement of the coastal front and evolution of the CAD have tremendous impacts on sensible weather in the region, including cloud cover, temperature, precipitation type and convective potential (Keeter et al. 1995).

It is hypothesized that a SF rainband can influence the evolution of the CAD and the coastal front. Several possibilities exist for SF/CAD interaction. Hydrostatic pressure falls from precipitation-induced latent heat release associated with a SF rainband crossing a saturated cold dome could influence the evolution of the cold dome and the coastal front. These pressure falls could also contribute to the formation of a mesoscale surface low in the Piedmont region. This impact would be highly dependent upon the placement of maximum latent heating in relation to the shape and size of the cold dome. In addition, it is hypothesized that evaporative cooling induced by a SF rainband could reinforce the CAD if it falls into an unsaturated cold dome. Again in this case, the timing and placement of the precipitation in the cold dome would be critical in determining the ultimate effects of the SF rainband.

In addition to the effects on the cold dome itself, the presence of the SF raises other forecast issues. Primary concerns include precipitation timing and severe convection. The timing of the SF rainband can be several hours ahead of what may be forecast as a rainband along the surface cold front. Also, due to the subsidence of dry air in the midlevels behind the SF, the passage of the surface cold front is often dry. There is also the possibility of elevated convection over the cold air or along the coastal front due to the potential instability created by advecting cool, dry air over the top of a warm, moist airmass that is present just above the top of the cold dome, e.g. Businger et al. (1991).

2. CASE OVERVIEW

The importance of the SF in a CAD event is demonstrated with the case of 13-14 February 2000. This event involved a well-defined SF and associated rainband that developed in the Southern Plains and moved across the southeastern U.S. The SF reached the Appalachians as a strong CAD event characterized by a saturated cold dome that was beginning to weaken. The SF rainband was associated with strong-to-severe convection as it moved across the Mississippi Valley and Gulf Coast. In addition, thunderstorms were observed as the SF passed over the CAD region on the

* *Corresponding author address:* Michael J. Brennan, North Carolina State University, Dept. of Marine, Earth and Atmospheric Sciences, Raleigh, NC 27695;
email: mike_brennan@ncsu.edu

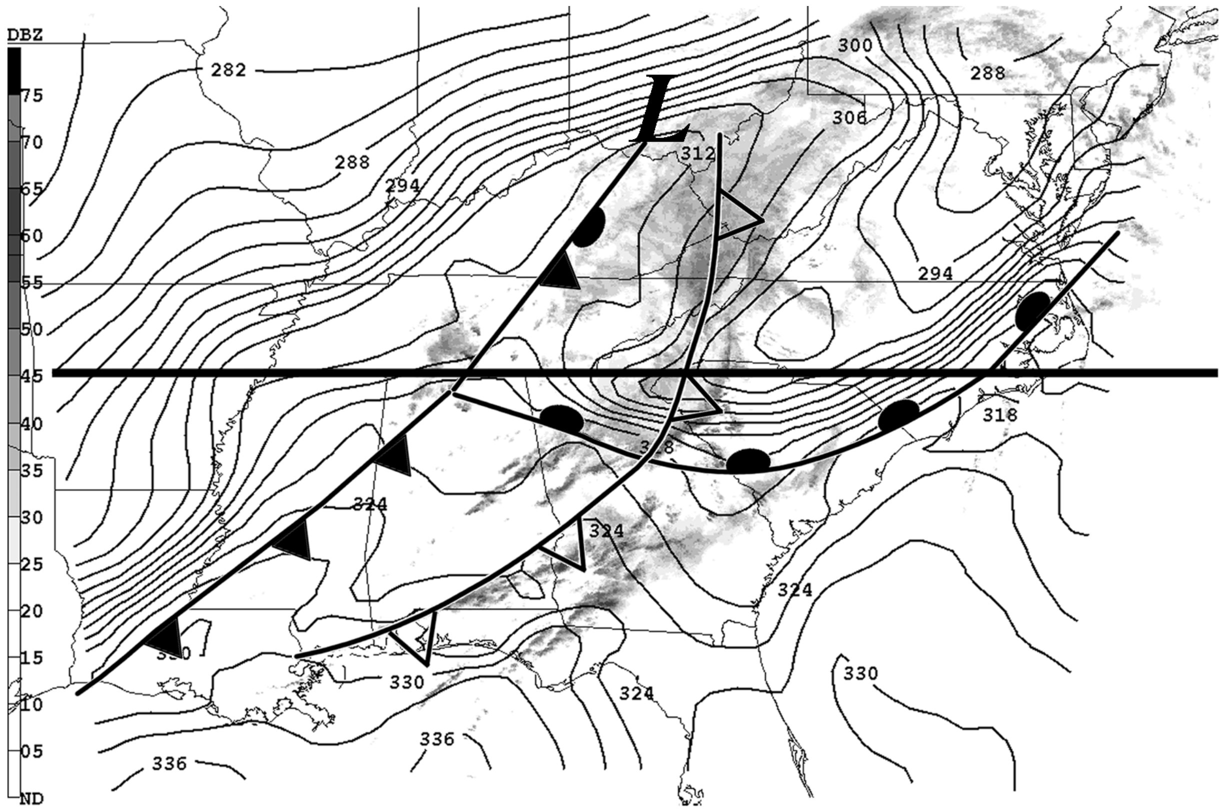

Fig. 1. Radar mosaic and MM5 forecast of surface equivalent potential temperature with analyzed surface and 700 hPa fronts, valid at 0600 UTC 14 Feb 2000. Surface fronts are shown with standard convention. Open barbs indicate the split front. The solid black line running horizontally across the image depicts the location of the cross-section displayed in Fig. 2.

evening of 14 February. Figure 1 shows a radar mosaic with a 6 h MM5 forecast of surface θ_e valid at 0600 UTC 14 February. Analyzed surface fronts and the 700 hPa SF have been drawn along with the cross section line used in Figure 2. At this time, the rainband runs from West Virginia to western North and South Carolina, across northern Georgia and ends in southern Alabama. There are also two separate rainbands on either side of the main band across eastern Alabama, southern Georgia and the Florida Panhandle. A 1001 mb surface low is in southern Ohio with an occluded front running across eastern Kentucky and Tennessee to a triple point in northern Alabama. The rainband is clearly well ahead of the surface occluded/cold front. The warm front extends from northern Alabama and northern Georgia and continues northeastward as a coastal front marking the southern and eastern edge of the CAD region. The SF is best indicated in the 700hPa equivalent potential temperature (θe) field. A 6 h forecast from the Eta model initialized at 0000 UTC 14 February (not shown) placed the SF in nearly the same location as that predicted by the MM5 model, though it was less well defined, probably because of its poorer grid resolution.

A cross-section of potential temperature (θ) and advection of θ_e from Amarillo, TX (AMA) to a point just offshore of Cape Hatteras, NC derived from the Eta model forecast valid at 0600 UTC 14 February is shown in Fig. 2. The separation between the surface cold front and the SF is revealed in both the potential temperature and θ_e advection fields. The surface front is indicated by the large static stability just to the west of the middle of the cross section, with cold θ_e advection taking place behind this feature at very low levels. A deep layer of cold θ_e advection present from 850 hPa to 300 hPa near the crest of the Appalachian Mountains is associated with the SF. The increased slope in the isentropes behind the leading edge of the cold advection also suggests the presence of the SF. The frontal locations inferred from the cross section are consistent with the indications from radar, surface observations and plots of forecast 700 hPa θ_e. Another notable feature is the CAD event ongoing east of the Appalachians. The coastal front is just onshore with strong warm θe advection occurring over the top of the cold dome inland of the coastal front.

By 1200 UTC, the SF had advanced across the remainder of the CAD region and was located along the coast, whereas the surface front was still along the Appalachians. By this time, the CAD had eroded considerably on its eastern and southern perimeter, with the warm/coastal front running along a Long Island, NY to Richmond, VA to Charlotte, NC line, effectively

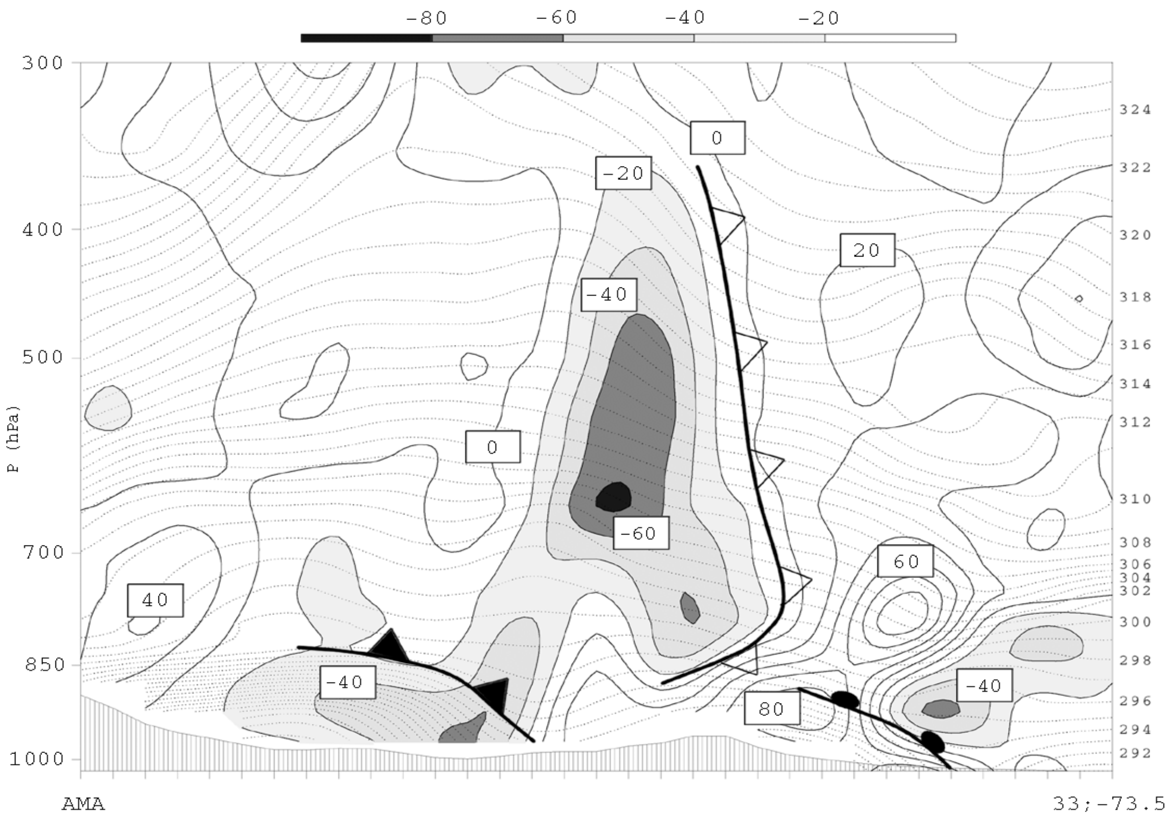

Fig. 2. Eta model cross section from Amarillo, TX to 33N 73.5W valid at 0600 UTC 14 Feb, showing isentropes (dotted) and advection of equivalent potential temperature (cold advection shaded). Fronts are as in Fig. 1.

squeezing the cold dome to an area just along and immediately east of the mountains. A thermal retrieval technique as described in Koch (2001) was applied to WSR-88D data from KRAX (Raleigh, NC) and KFFC (Atlanta, GA) radars. Both analyses indicated a large area of geostrophic cold advection following the passage of the SF rainband ahead of the surface cold front (to be shown at the conference).

3. IMPACTS OF THE SPLIT FRONT ON CAD EVOLUTION

As the SF rainband passed over the CAD region, reported 6 h precipitation totals ranged from ~10mm to > 20mm. Parameterized latent heat calculations via the method described in Emanuel et al. (1987) were made from Eta model grids every six hours. Following this method, latent heat is computed throughout the Eta model domain using the following equation

$$\frac{dq}{dt} = w\left(\frac{\partial q}{\partial p} - \frac{g_m}{g_d}\frac{q}{q_e}\frac{\partial q_e}{\partial p}\right)$$

where w is vertical motion, g_d is the dry adiabatic lapse rate and g_m is the moist adiabatic lapse rate. These calculations indicate a large area of latent heat released in the 700 hPa – 400 hPa layer with the passage of the SF rainband across the CAD region between 0600 and 1200 UTC 14 February (not shown). This agrees well with the timing of observed precipitation at the ground and radar trends. Objective analysis of three hourly surface data (Fig. 3) showed that a large area of significant surface pressure falls moved along with the SF rainband as it propagated from the northern Gulf Coast states, across the Appalachians and into the Carolinas. Three hourly pressure falls from 0300 to 0600 UTC reached a maximum magnitude of 6 hPa near Charlotte, NC. Kinematic surface frontogenesis computed using both the total wind and the isallobaric wind showed significant frontogenesis occurred along the eastern margin of the cold dome as the SF advanced across the region. For example, the strongest frontogenesis at 0600 UTC displayed a maximum of total frontogenesis along the North Carolina/South Carolina border, with isallobaric frontogenesis maximized near Augusta, GA and another maximum located in northwestern NC. The impact of these frontogenetical areas is the subject of ongoing research. Other ongoing investigations include an MM5

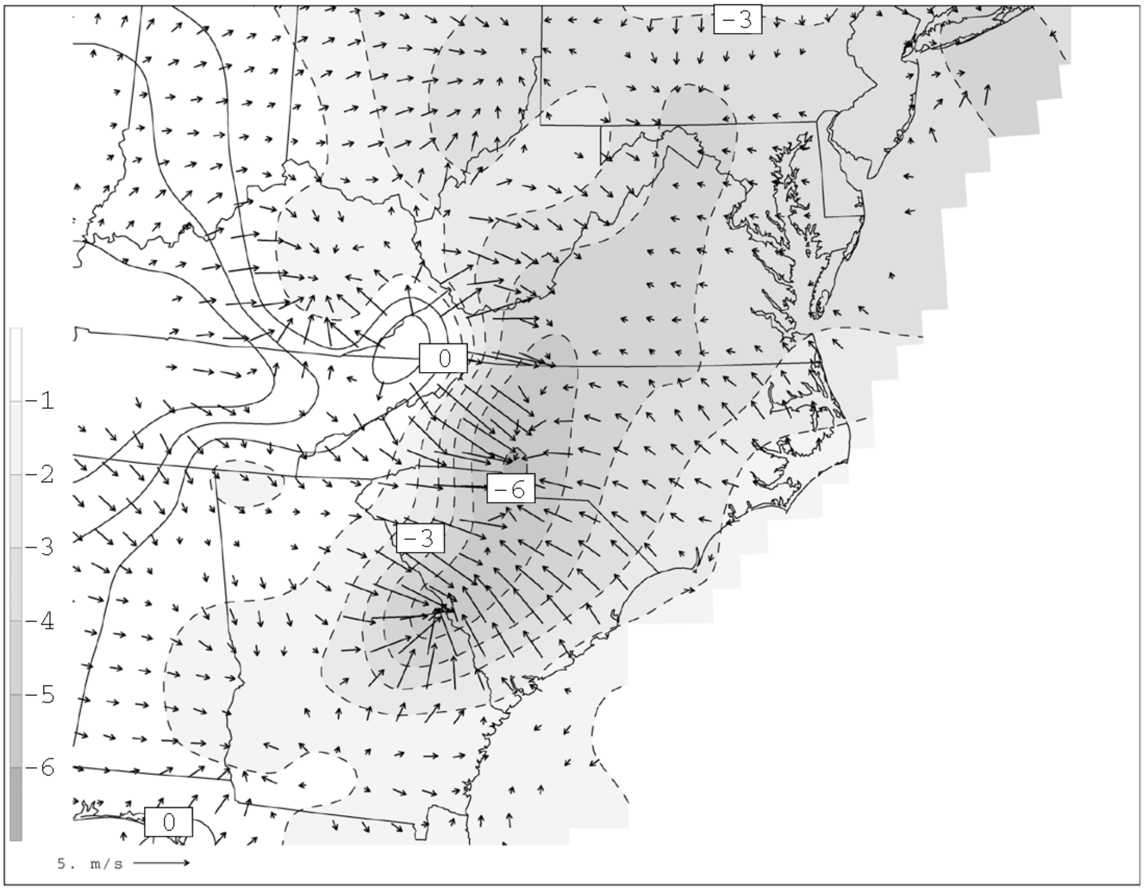

Fig. 3. Objective analysis of 3-hour pressure change (pressure falls shaded) and resulting isallobaric wind at 0600 UTC 14 February.

simulation of this case to investigate the influence of latent heat release in the SF rainband on the CAD evolution. After successfully simulating the CAD and SF evolution with a control run, a run with no latent heat was made to assess how the CAD and SF would have evolved differently without the impact of latent heat release from the SF rainband. Results from a comparison of the two simulations indicate that latent heat was critical to the narrowing and erosion of the CAD and that the forecast isallobaric field was governed by this diabatic heating. The inference is that diabatically-forced isallobaric frontogenesis led to the demise of the CAD region. In addition, with the higher resolution data set from the MM5 forecasts we will investigate the vertical circulation associated with the isallobaric frontogenesis at the top of the CAD dome. The objective here is to try to quantify its effects relative to that of the ongoing warm advection above the cold dome in affecting the evolution of CAD.

5. ACKNOWLEDGEMENTS

This research was funded by NOAA CSTAR grant NA-07WA0206NSF and NSF grant ATM-9700626. Special thanks are due to Kermit Keeter and Ruth Aiken of the Raleigh National Weather Service office who were extremely helpful in obtaining the Level II NEXRAD data used in this study. Also, we acknowledge Mike Trexler for his invaluable assistance with the graphics.

6. REFERENCES

Bell, G. D., and L. F. Bosart, 1988: Appalachian cold air damming. *Mon. Wea. Rev.*, **116,** 137-161.

Bosart, L. F., C. J. Vaudo, and J. H. Helsdon, Jr., 1972: Coastal frontogenesis. *J. Appl. Met.*, **11,** 1236-1258.

Browning, K. A., and G. A. Monk, 1982: A simple model for the synoptic analysis of cold fronts. *Quart. J. Roy. Meteor. Soc*., **108,** 435-452.

Businger, S. W., W. H. Baumann III, and G. F. Watson, 1991: The development of the Piedmont front and associated outbreak of severe weather on 13 March 1986. *Mon. Wea. Rev.*, **119,** 2224-2251.

Emanuel, K. A., M. Fantini, and A. J. Thorpe, 1987: Baroclinic instability in an environment of small stability to slantwise moist convection. Part I: Two-dimensional models. *J. Atmos. Sci.* **44,** 1559-1573.

Forbes, G. S., R. A. Anthes and D.W. Thompson, 1987: Synoptic and mesoscale aspects of an Appalachian ice storm associated with cold-air damming. *Mon. Wea. Rev*., **115,** 564-591.

Fritsch, J. M., J. Kapolka, and P. A. Hirschberg, 1992: The effects of subcloud-layer diabatic processes on cold air damming. *J. Atmos. Sci.*, **49,** 49-70.

Hobbs, P. V., J. D. Locatelli, and J. E. Martin, 1990: Cold fronts aloft and the forecasting of precipitation and severe weather east of the Rocky Mountains. *Wea. Forecasting*, **5,** 613-626.

Keeter, K. K., S. Businger, L. G. Lee, J. S. Waldstreicher, 1995: Winter weather forecasting throughout the eastern United States. Part III: The effects of topography and the variability of winter weather in the Carolinas and Virginia. *Wea. Forecasting,* **10,** 42-60.

Koch, S. E., 2001: Real-time detection of split fronts using mesoscale models and WSR-88D radar products. *Wea. Forecasting*, **16,** 35-55.

Koch, S. E., and Mitchem, J., 2001: The role of dual cold fronts aloft in a major tornado and flash flooding event. *Precipitation Extremes: Prediction, Impacts, and Responses,* Albuquerque, NM, Amer. Meteor. Soc., 180-184.

Locatelli, J. D., M. T. Stoelinga, and P. V. Hobbs, 1998: Structure and evolution of winter cyclones in the central United States and their effects of distribution of precipitation. Part V: Thermodynamic and dual-Doppler radar analysis of a squall line associated with a cold front aloft. *Mon. Wea. Rev*., **126,** 860-875.

Riordan, A. J., 1990: Examination of the mesoscale features of the GALE coastal front of 24-25 January 1986. *Mon. Wea. Rev.*, **118,** 258-282.